

On the efficiency roll-off in Perovskite Light Emitting Diodes

Pradeep R. Nair* and Advait Kiran Marathi
*Department of Electrical Engineering,
Indian Institute of Technology Bombay, Mumbai, India*

(Dated: July 31, 2025)

Here, we report a comprehensive modeling framework to unravel the efficiency roll-off in Perovskite light emitting diodes (PeLEDs). Our model self-consistently accounts for a positive feedback mechanism which involves diverse phenomena like temperature-dependent carrier recombination, space charge effects, Joule heating, and thermal transport. Model predictions compare well with experimental results such as dark current-voltage characteristics and efficiency as well as radiance roll-off under high injection conditions. This work identifies key performance limiting phenomena in current state-of-the-art PeLEDs and could be of broad relevance towards device optimization, thermal design, packaging, and operational lifetime.

I. INTRODUCTION

Perovskite based light emitting diodes (LEDs) have achieved impressive progress in the recent years [1–6]. Reports indicate external quantum efficiency (EQE) over 30% [6, 7], and high color purity [8]. It is possible to tune emission over a broad spectra by changing the halide composition (and hence the band gap) [9]. Due to their excellent electroluminescence properties, Photoluminescence Quantum Yield (PLQY) of halide perovskites has been quite high ($> 90\%$) [6, 8]. In addition, high defect tolerance and solution processibility of perovskites contributes to streamline fabrication process [9]. Attempts to enhance the performance of PeLEDs include facilitating efficient injection of charge carriers from the transport layers, increasing radiative recombination within the active region, and improving light extraction from the substrate [10]. Despite these encouraging improvements, stability remains a major challenge towards successful commercialization [9].

For energy-efficient display applications, it is important to achieve high radiance output under low power consumption. Rather, excellent EQE should be demonstrated for large injection conditions (i.e., in terms of the input current). However, initial reports indicate PeLEDs suffer from EQE roll-off (or droop) at high injection levels [6, 10]. This critical phenomenon is not yet fully understood in terms of the functional dependence of key associated parameters. As a result, there exist several open questions related to the design, optimization, and stability of PeLEDs. To list a few: (a) What causes EQE roll-off in PeLEDs? (c) Is there a consistent explanation for the decrease in radiance at high injection levels? and (c) How does power dissipation and associated Joule heating contribute to efficiency roll-off? and (d) What are the optimization pathways?

Here, we provide a comprehensive modeling framework to address the above open questions. Specifically, we unravel the influence of the coupled electrical, thermal, and radiative mechanisms on the operation of PeLEDs. Through this, we predict important features like current (J) - Voltage (V) characteristics, EQE vs. J , energy conversion efficiency (ECE) vs. J , radiance vs. power consumption, etc. Our model predictions compare well with recent experimental results. This calibrated model allows us to explore the key mechanisms involved in EQE as well as radiance roll-off in PeLEDs. Curiously, in contrast to the conventional view, here we find that Auger recombination and Joule heating on its own are not the major contributors towards EQE roll-off. On the other hand, a positive feedback mechanism which involves Joule heating and temperature dependence of radiative recombination is the dominant factor that causes efficiency droop in PeLEDs. This help us identify key strategies for further device optimization. Below we first describe a multi-physics model and then compare it against experimental results.

II. MULTI-PHYSICS MODEL

The key performance parameters of a LED are the quantum efficiency, radiance, and the associated power consumption. As such, the main optimization challenge is to achieve the desired radiance with minimum power consumption over the stipulated lifetime. To address this optimization challenge, it is imperative to have predictive models for EQE as a function of injection current. To this end, we need a reasonable description of the JV characteristics and the associated radiative recombination. In this regard, our recent work on photoluminescence (PL) in Perovskites showed that a major factor which contributes to the PL efficiency roll-off (or droop) is the positive feedback mechanism between the laser induced temperature (T) increase of the sample and the temperature dependence of radiative recombination [11]. Indeed, similar aspects

* prnair@ee.iitb.ac.in

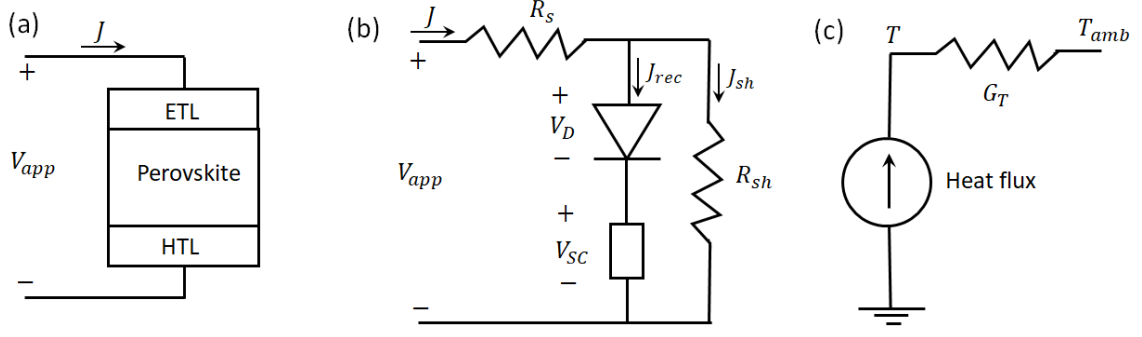


FIG. 1. Multi-physics model for Perovskite LEDs. (a) Schematic of PeLED. (b) Equivalent circuit description for the electrical characteristics (as described by eqs. 1-7). Here, the applied bias supports the potential drop across R_s and facilitates carrier recombination along with space charge limited transport in the LED. R_{sh} denotes the shunt resistance. Part (c) shows the equivalent circuit to analyze the heat transport in terms of the power dissipation and effective thermal conductance G_T (as described by eq. 8).

could be relevant for LEDs as well. During operation, the temperature of the active layer could increase due to Joule heating which could influence the efficiency of radiative recombination and hence the EQE roll-off.

In this section, we describe a self-consistent model that accounts for the JV characteristics of the device, temperature increase due to Joule heating, and the associated temperature dependence of radiative recombination. For this, we consider a simple PeLED structure with the active layer sandwiched between transport layers (TL, see part (a) of Fig. 1). The carrier transport in PeLEDs can be quite complex and is influenced by phenomena like recombination, space charge effects, ion migration, etc. [12, 13] Although these phenomena are inherently coupled to each other, a compact description of the J-V characteristics is possible through an equivalent circuit representation as given in Fig. 1b.

With sufficient electron and hole blocking barriers in the respective transport layers (see Fig. 1a), the current is limited by recombination in the active layer [12, 14]. Accordingly, the recombination current (J_{rec} , see Fig. 1b) is given as

$$J_{rec} = q(k_1 n + k_2 n^2 + k_3 n^3)W_P \quad (1)$$

where q is the electronic charge and W_P is the thickness of the Perovskite active layer. This equation assumes that $n = p$, where n and p are the electron and hole densities, respectively. The parameters k_1 , k_2 , and k_3 account for mono-molecular, bimolecular, and Auger recombination, respectively.

It is well known that recombination processes are temperature (T) dependent [15]. For the temperature range of interest ($300 \text{ K} < T < 350 \text{ K}$), we recently showed that the temperature dependence of radiative recombination can be represented as [11]

$$k_2 = k_{2,F} e^{E_A/kT} \quad (2)$$

Here E_A is the activation energy, $k_{2,F}$ is the pre-factor, k is the Boltzmann's constant, and T is the temperature of the active layer. Among the several factors, the temperature dependence of refractive indices (or absorption coefficients) significantly contributes to the E_A . Using the well known von Roosbroeck-Shockley model [16], our analysis indicates that E_A could be of the order of 100 mV - which is supported by transient absorption measurements [17]. More details on the temperature dependence of k_2 is available in our recent publication [11].

The applied voltage (V_{app}) drops across series resistance (R_s , if any) and the PeLED (see Fig. 1b). The potential drop across the PeLED should support both carrier recombination and space charge limited transport. To a first order, this could be visualized in terms of the drop across the active layer (V_D , and represented by the diode in Fig. 1b) and the potential needed to support the space charge limited carrier transport (V_{SC}). With the assumptions of active layer being undoped, $n = p$, and negligible drop in the quasi-Fermi levels, we have

$$V_D = \frac{2kT}{q} \ln\left(\frac{n}{n_i}\right) \quad (3)$$

where n_i is the intrinsic carrier density. Although a single diode is shown in the schematic in Fig. 1b for ease of representation, it is evident from eq. 1 and eq. 3 that it requires 3 diodes with distinct ideality factors to represent the recombination current [14].

Under steady state conditions, the current through the active layer and the transport layers remains the same. While the magnitude of current is governed by the carrier recombination in the active layer, space charge effects could dictate the carrier transport and hence the net potential drop across the PeLED. Accordingly, in general terms, the potential drop required to support the space

charge limited current is given by [18, 19]

$$V_{SC} = K_{SC} J_{rec}^\alpha \quad (4)$$

where the exponent α could be influenced by the specific nature of trap distribution. We note that a wide range of values (both theoretical and experimental) for α is reported in the literature [20]. Among others, the pre-factor K_{SC} is determined by parameters like mobility, dielectric constant, and effective thickness of the space charge region, etc.

Using the equivalent circuit, Fig. 1b, the current voltage characteristics (J vs. V_{app}) and the power drawn from the external source (P) can now be expressed in terms of the various components as

$$J = J_{rec} + (V_D + V_{SC})/R_{sh} \quad (5)$$

$$V_{app} = V_D + V_{SC} + J R_s \quad (6)$$

$$P = J V_{app} \quad (7)$$

The active layer temperature is expected to increase due to Joule heating during LED operation. Of the input power of $J V_{app}$, only a certain fraction is converted to photons which results in light emission. The rest of the input power is dissipated as heat and the thermal conduction through the various layers (which includes packaging) determines the temperature of the active layer.

The temperature of the active layer can be effectively estimated using the thermal equivalent circuit shown in Fig. 1c. As the net radiative recombination in the LED is nothing but $k_2 n^2 W_P$, the corresponding power density of the light emission is given as $k_2 n^2 W_P \times q E_g \times \eta_{OC}$, where η_{OC} is the light out-coupling factor (here we assume that all emitted photons are with energy E_g , the band gap). The net power (P) delivered by the external source to the LED is $P = J V_{app}$. Accordingly, continuity of the heat flux under steady-state conditions leads us to

$$G_T (T - T_{amb}) = J V_{app} - q k_2 n^2 W_P E_g \times \eta_{OC} \quad (8)$$

where T_{amb} is the ambient temperature, and G_T is the effective thermal conductance.

Eq. 8 describes the balance of heat flux in a PeLED. Here, the term on the LHS is the net heat flux from the LED to the ambience, while the RHS denotes the net heat flux generated under electrical injection. Eq. 8 assumes that thermal conduction is the main heat transport mechanism, and electrical power dissipation or thermal heat generation happens in the sandwich structure of PeLED (see Fig. 1a). Subsequent heat transport occurs through the various layers (including packaging) to the ambient environment (also see Fig. 1c). Accordingly, the parameter G_T is the effective thermal conductance which depends on several factors such as thickness and thermal conductivity of various

layers, interface thermal resistance [21], etc. A similar compact model successfully explained the thermal aspects in thin-film Perovskites under steady state PL measurements [11].

The performance parameters of PeLEDs are defined as follows: The internal quantum efficiency (IQE) is defined as the fraction of injected carriers which undergo radiative recombination and is given as

$$IQE = \frac{k_2 n^2 W_P}{J/q} \quad (9)$$

while the external quantum efficiency (EQE) is given as

$$EQE = IQE \times \eta_{OC} \quad (10)$$

The energy conversion efficiency (ECE, or the Wall Plug efficiency) is the fraction of the input power which is emitted as light. With input power given by eq. 7, and under the assumption that all emission happens at the band-edge, the ECE is given as

$$ECE = \frac{q k_2 n^2 E_g W_P \times \eta_{OC}}{J \times V_{app}} \quad (11)$$

The radiance (Φ_{rad}) in terms of emitted power per unit area per solid angle under the assumption of single sided emission (with perfect reflection from the other side) is given as

$$\Phi_{rad} = k_2 n^2 W_P \times q E_g \times \eta_{OC} / \theta \quad (12)$$

where the factor θ is the effective solid angle to which a small LED can emit photons.

III. RESULTS AND DISCUSSIONS

Equations 1 -12 provide a self-consistent description of PeLEDs. It accounts for various phenomena like carrier recombination, space charge effects, power dissipation, heat transport, and associated decrease in the radiative recombination efficiency. Numerical solution (Newton-Raphson method) of eqs. 1-8 leads to self consistent estimates for n , T , and J for a given V_{app} . This allows us to estimate the performance parameters as per eqs. 9 - 12. Under large electrical injection, the power dissipation leads to an increase in T (see eq. 8) which leads to a decrease in k_2 (as per eq. 2). Any reduction in k_2 in turn increases the power dissipation which leads to an increase in temperature (see eq. 8). Indeed, this is a positive feedback mechanism which leads to an increase in temperature that contributes to a reduction in radiative recombination and hence to the efficiency roll-off under high injection conditions.

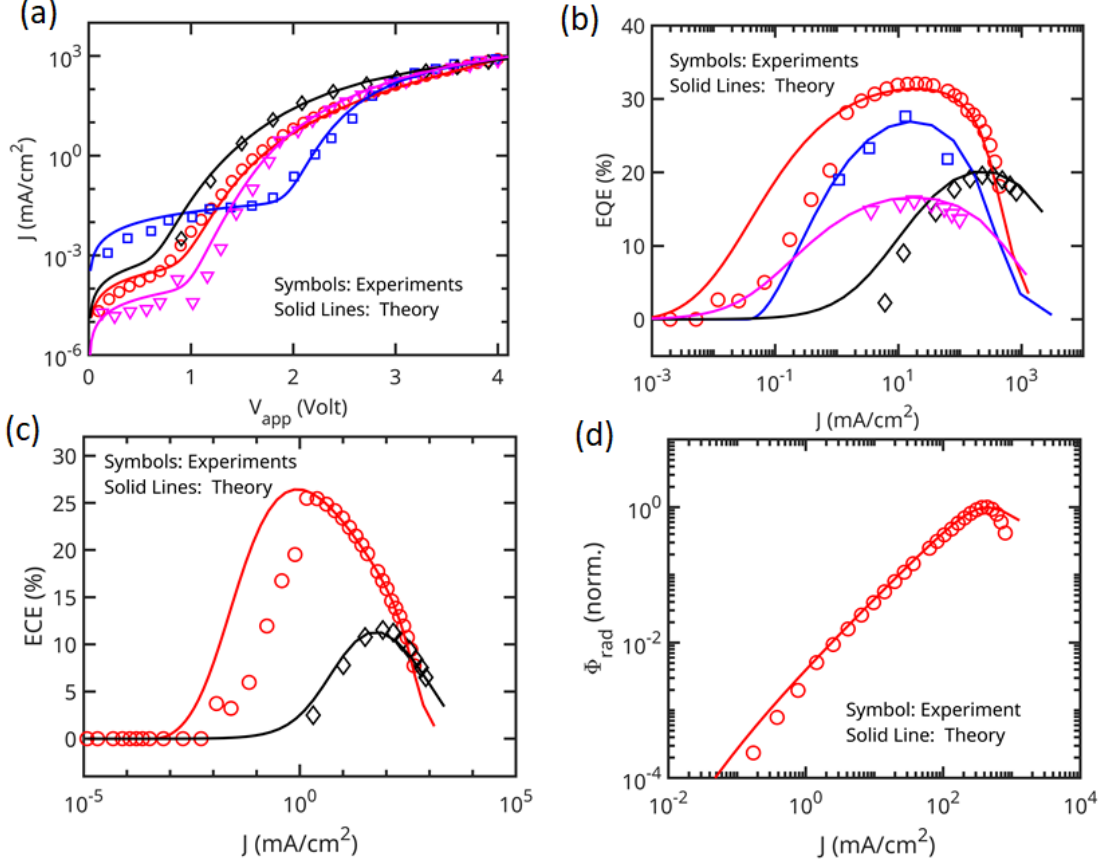


FIG. 2. Comparison of model predictions with experimental results. The symbols represent experimental results from literature while the lines are model predictions (a) Dark $J - V$ characteristics of PeLED, (b) EQE, (c) ECE, and (d) radiance. The experimental results and corresponding references are: red circles (ref. [6]), black diamonds (ref. [10]), magenta triangles (ref. [22]), and blue squares (ref. [23])

Detailed comparisons between model predictions (i.e., numerical solutions of eqs. 1-12) and experimental results are provided in Fig. 2. The experimental results are from recent publications [6, 10, 22, 23]. The experimental results are dark $J - V$ (part (a), 4 data sets), EQE vs. J (part (b), 4 data sets), ECE vs. J (part (c), 2 data sets) and Φ_{rad} vs. J (part (d), 1 data set). We find several common trends in these experimental results, even though they are from different laboratories, with different active layers of perovskites (E_g ranging from 1.4 – 2.42 eV) and different processing conditions. To list a few: (i) low bias regime of J vs. V_{app} shows influence of shunt resistance, (ii) diode like features in J vs. V_{app} in the medium bias regime, (iii) nearly similar sub-exponential increase in J for large V_{app} (Fig. 2a), (iv) a broad peak in both EQE vs. J and ECE vs. J followed by roll-off, and (v) a near linear increase in radiance with J followed by its roll-off under high injection conditions (Fig. 2d).

Model predictions are shown as solid lines in Fig. 2. Indeed, all the key trends in experimental results are well anticipated by our proposed model, which validates

the multi-physics approach. The parameters used in this study are listed in Table I. The parameters used in the model predictions for the experimental results from ref. [6] (i.e., data set shown in red color, Fig. 2) are based on a self-consistent analysis of the corresponding time resolved Photoluminescence (TRPL) transients (as recently reported [24]). We find that model predictions indicate that the parameters related to recombination kinetics (k_1, k_2, k_3), light out-coupling factor (η_{OC}), space charge limited transport (k_{SC}, α) etc. are comparable in their relative magnitudes, with some key distinct trends, across the different experimental data sets.

Several noteworthy insights are readily available in the results shared in Fig. 2, as discussed below.

A. Efficiency roll-off and Joule heating: An important tradeoff associated with LEDs is the desired light output and associated power consumption. The same is usually discussed in terms of efficiency roll-off under high injection conditions. The results shown in Figs. 2b,c show that the proposed model compares well with the EQE as well as ECE characteristics

Parameter	Units	Fig. 2: Data sets			
		Model: red line, Exp: red circles, ref. [6]	Model: black line, Exp: black dia- monds, ref. [10]	Model: magenta line, Exp: magenta trian- gles, ref. [22]	Model: blue line, Exp: blue squares, ref. [23]

TABLE I. Parameters used in model predictions in Fig. 2. Here, E_g and W_P for each data set are as reported in the respective references. The recombination parameters used in the analysis of experimental results from ref. [6] are based on an analysis of corresponding experimental TRPL data (ref. [25])

of experimental results. For LEDs limited by carrier recombination, the low bias current could be dominated by monomolecular recombination (with $J \propto k_1 n$) while bimolecular recombination dominates the mid-bias regime (with $J \propto k_2 n^2$). Under large biases, the current could be dominated by Auger recombination (with $J \propto k_3 n^3$). Accordingly, it can be shown that the EQE first increases linearly with n , then it may remain fairly independent of n and finally the EQE will vary as n^{-1} . In terms of J , we expect the EQE to first increase with J , then remain invariant with J , and finally decrease as $J^{-1/3}$. Hence, EQE roll-off is a fundamental characteristic expected in all LEDs where the current is limited by carrier recombination.

The EQE roll-off in PeLEDs is often attributed to Joule heating effects - in addition to the above discussed influence of Auger recombination. Our model provides interesting quantitative insights in this regard. Figure 3 compares the influence of Joule heating and temperature dependence of k_2 on the EQE roll-off. Here, the symbols represent simulation results at room temperature - i.e., in the absence of any Joule heating effects with k_2 being a constant. The EQE roll-off in this case is entirely due to Auger recombination being the dominant mechanism under high injection conditions. The blue line shows simulation results in the presence of Joule heating but with k_2 being temperature independent. Surprisingly, we find that the EQE roll-off remains unchanged in this case. This indicates that Joule heating, on its own, does not contribute to any additional roll-off in EQE . This is expected as EQE in the absence of shunt paths (see eq. 10) depends only on the recombination parameters and η_{OC} . With these parameters being temperature independent, Joule heating is not expected to contribute to EQE roll-off. On the other hand, with k_2 being temperature dependent, we find that EQE roll-off is significantly affected (see red line in Fig. 3 which is also the same data plotted in Fig. 2b). Hence, EQE roll-off in PeLEDs is caused by a combination of Joule heating, the temperature dependence of k_2 , and increased Auger recombination (and not by a stand alone effect or a combined effect of Joule heating and Auger recombination).

B. Radiance roll-off and leakage currents: Our model helps to delineate the role of parasitic elements, such as leakage paths, in the PeLED characteristics.

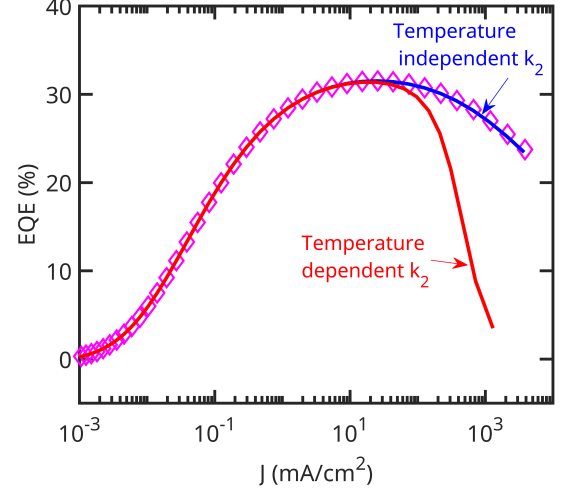


FIG. 3. Influence of Joule heating on EQE roll-off. The symbols represent simulation results under room temperature operation (i.e., $T = 298K$). Here the roll-off is entirely due to Auger recombination. Blue line indicates EQE roll-off in the presence of Joule heating with k_2 being temperature independent. The red line indicate EQE roll-off in the presence of Joule heating with temperature dependent k_2 . These results indicate that Joule heating on its own do not have any significant contribution to EQE roll-off. In fact, EQE roll-off is dominated by the Joule heating induced reduction in k_2 . The parameters used are the same as the data set indicated by red lines and symbols in Fig. 2.

The influence of simple shunt resistances is often directly evident from the $J - V$ characteristics (see Fig. 2a). However, it is possible to have several parasitic effects which are more complex than simple shunt resistances. For example, the energy band offsets or barriers between the transport layers and the active layer might not be large enough. Here, the carriers injected from one TL could reach the other TL without undergoing recombination. Such undesired over-the-barrier transport of carriers also contributes to J and hence to the EQE roll-off under high injection conditions. Can the proposed formalism be used to ascertain and quantify the influence of such non-ohmic parasitic components? Rather, what signature could unambiguously distinguish between the power dissipation-induced temperature increase and its after effects against parasitic leakage paths?

The key to unravel the above puzzle lies in the scaling trends of radiance (and not the *EQE* roll-off). As J increases, the radiance of a LED, which depends only on the radiative recombination, is expected to increase monotonically (it may saturate, in some limiting scenarios). This trend is expected even in the presence of additional undesired over-the-barrier transport of carriers. The radiance can decrease only if there is a decrease in n or k_2 or both. Typically, any decrease in n will also lead to a decrease in J (both recombination and parasitic components). Hence, an experimental observation of a decrease in radiance with an increase in J can happen only if k_2 decreases under high injection conditions (unless dominant non-radiative recombination pathways are newly activated through material degradation or otherwise). The same is predicted by our model and is seen in experiments as well (see Fig. 2d). Hence, instead of the *EQE*, the radiance vs. J trends could provide unambiguous evidence on the underlying physical mechanism that govern the PeLED operation under high injection conditions - leakage paths vs. a positive feedback involving power dissipation, heat transport, and reduced radiative recombination.

C. Optimization pathways: Our results identify an important performance limiting bottleneck in some of the recent PeLEDs. As indicated by Fig. 2 and Table I, the ON characteristics is dominated by space charge limited transport. This increases the operating voltage V_{app} required to achieve significant radiance. The corresponding power dissipation increases temperature which contributes to an reduction in k_2 and hence the *EQE* roll-off. Hence, the most important optimization pathway for PeLEDs is to improve the transport properties - both electronic and thermal. This will aid to achieve high radiance with reduced power consumption. Of course, improvement in material quality (i.e., reduced k_1) is also a desired feature.

The increase in active layer temperature and the associated decrease in k_2 are central to *EQE* roll-off. This reduction in k_2 could be due to either E_A or T or both (see eq. 2). Eq. 8 indicates that T is significantly influenced by G_T . Accordingly, the variables that dictate the *EQE* roll-off are E_A and G_T . Larger E_A or smaller G_T leads to a significant reduction in k_2 and hence increases the *EQE* roll-off. This indicates the importance of characterizing the temperature dependence of the recombination parameters and appropriate thermal design for PeLEDs.

D. Dark JV Characteristics: Figure 2a indicate that the dark JV characteristics share some common features. For example, the low bias regime of all devices show evidence of shunt resistances over a broad range of values (i.e., over two orders of magnitude, see Table I). The turn-ON characteristics (i.e., with

diode-like exponential increase in current with V_{app}) shows significant variation. However, the same is consistent with the variation of n_i with E_g . As the E_g increases, n_i decreases exponentially and hence the V_{app} required to turn the device ON increases (as per eq. 3). The back extracted values for n_i in Table I varies almost exponentially with E_g (the deviations could be attributed to the differences in the effective density of states of the respective materials). The high bias regime of all devices shows similar trends; however, these are not limited by series resistance effects. On the other hand, these characteristics are well described by the space charge effects (i.e., eq. 4) and the corresponding parameters (K_{SC} and α) are similar for all devices - a surprising result as these devices have different materials, structures, processing conditions, etc. We find $\alpha = 0.25$, which is consistent with the literature [20, 26]. Future research could explore device architectures to reduce the operating voltages and hence power consumption.

Overall, here we developed a coherent theoretical framework for PeLEDs which accounts for several critical phenomena like temperature dependent carrier recombination, space charge limited carrier transport, thermal dissipation, heat transport, and a positive feedback mechanism which involves all of the above. As a result, our model anticipates several key features of PeLEDs (with band gaps ranging from 1.4 – 2.42 eV), and elucidates the scope and pathways for further optimization. The model predictions are indeed subject to the parameters used. Here, the recombination parameters associated with one data set (shown in blue, Fig. 2) were back extracted from the corresponding TRPL data (see ref. [25]). Of the various parameters listed in Table I, k_1 , k_2 , and k_3 dictate the carrier recombination while K_{SC} , α , R_s , R_{sh} , etc. influences the transport characteristics (i.e., large bias dark $J - V$). Accordingly, our simulations indicate that small changes in α lead to distinct changes in the $J - V$ characteristics (with insignificant changes in *EQE* vs. J characteristics, see Fig. S1, Suppl. Mat.), while *EQE* and *ECE* are very sensitive to even minor changes in recombination parameters (with negligible changes in $J - V$ characteristics, see Fig. S2, Suppl. Mat.). As such, this highlights a unique aspect about the proposed model: We describe several features (i.e. JV , *EQE*, *ECE*, radiance, etc.) with contrasting dependence on key functional parameters through a coherent modeling framework which establishes the validity of both the methodology and the parameters used. Additional details on the variation of V_D , n , and T as a function of V_{app} are provided in Fig. S3, Suppl. Mat. We also note that the parameters T and E_A have a combined effect on the device characteristics. Similar amount of *EQE* roll-off can be obtained for a lower increase in T , but with a larger E_A and vice-versa.

It is well known that PeLEDs (and solar cells) could be influenced by aspects like ion migration, band level

offsets, interface recombination, etc. The influence of the same on solar cells has been addressed in several of our prior publications [13, 27–29]. In particular, the assumption $n = p$ in the active layer might not be appropriate under all scenarios [10]. However, the same holds in the presence of significant mobile ions and hence the insights shared are relevant for such cases. We note that our model overestimates EQE and ECE for low J values (see Fig. 2b,c). This is not a major concern as such low current levels (i.e., $J < 1 \text{ mA/cm}^2$) are not of practical significance. A possible physical origin for this mismatch is explored through numerical simulations in Suppl. Mat. (dependence on mobile ions, see Fig. S4). Further, experimental results indicate that the radiance roll-off at very high injection conditions is more than the model predictions (see Fig. 2d). Several non-idealities including material degradation and hence an increase in non-radiative recombination could be relevant at such extreme high injection conditions. In addition, the power dissipation and associated thermal analysis provided in this manuscript could be relevant for modeling the operational lifetime of PeLEDs in view of various degradation mechanisms such as phase segregation[29], trap generation, grain boundary effects, etc. Our results also have obvious implications towards back extraction of recombination parameters from *EQE* characteristics of PeLEDs.

IV. CONCLUSIONS

In summary, here we report a comprehensive modeling methodology to identify key performance limiting factors of PeLEDs. Our analysis shows that undesired power dissipation due to space charge effects and associated thermal management issues leads to a temperature increase in the active layer. In addition, a positive feedback mechanism between heat transport and temperature dependence of radiative recombination results in several important features, such as efficiency and radiance roll-off under high injection conditions. As such, this manuscript provides a multi-physics description of PeLEDs with key performance limiting factors identified, paving the way for further optimization.

V. ACKNOWLEDGEMENTS

The authors acknowledge National Center for Photovoltaics Research and Education (NCPRE), Indian Institute of Technology Bombay. The authors also acknowledge discussions with Simhadri Venkata Ramana, and Sushama Usurupatti, IIT Bombay

REFERENCES

-
- [1] J. J. Yoo, G. Seo, M. R. Chua, T. G. Park, Y. Lu, F. Rotermund, Y.-K. Kim, C. S. Moon, N. J. Jeon, J.-P. Correa-Baena, V. Bulović, S. S. Shin, M. G. Bawendi, and J. Seo, Efficient perovskite solar cells via improved carrier management, *Nature* **590**, 587 (2021).
 - [2] Z. Shen, Q. Han, X. Luo, Y. Shen, Y. Wang, Y. Yuan, Y. Zhang, Y. Yang, and L. Han, Efficient and stable perovskite solar cells with regulated depletion region, *Nature Photonics* **18**, 450 (2024).
 - [3] Y. Sun, L. Ge, L. Dai, C. Cho, J. Ferrer Orri, K. Ji, S. J. Zelewski, Y. Liu, A. J. Mirabelli, Y. Zhang, J.-Y. Huang, Y. Wang, K. Gong, M. C. Lai, L. Zhang, D. Yang, J. Lin, E. M. Tennyson, C. Ducati, S. D. Stranks, L.-S. Cui, and N. C. Greenham, Bright and stable perovskite light-emitting diodes in the near-infrared range, *Nature* **615**, 830 (2023).
 - [4] J. S. Kim, J.-M. Heo, G.-S. Park, S.-J. Woo, C. Cho, H. J. Yun, D.-H. Kim, J. Park, S.-C. Lee, S.-H. Park, E. Yoon, N. C. Greenham, and T.-W. Lee, Ultra-bright, efficient and stable perovskite light-emitting diodes, *Nature* **611**, 688 (2022).
 - [5] J. Liu, Y. He, L. Ding, H. Zhang, Q. Li, L. Jia, J. Yu, T. W. Lau, M. Li, Y. Qin, X. Gu, F. Zhang, Q. Li, Y. Yang, S. Zhao, X. Wu, J. Liu, T. Liu, Y. Gao, Y. Wang, X. Dong, H. Chen, P. Li, T. Zhou, M. Yang, X. Ru, F. Peng, S. Yin, M. Qu, D. Zhao, Z. Zhao, M. Li, P. Guo, H. Yan, C. Xiao, P. Xiao, J. Yin, X. Zhang, Z. Li, B. He, and X. Xu, Perovskite/silicon tandem solar cells with bilayer interface passivation, *Nature* (2024).
 - [6] M. Li, Y. Yang, Z. Kuang, C. Hao, S. Wang, F. Lu, Z. Liu, J. Liu, L. Zeng, Y. Cai, Y. Mao, J. Guo, H. Tian, G. Xing, Y. Cao, C. Ma, N. Wang, Q. Peng, L. Zhu, W. Huang, and J. Wang, Acceleration of radiative recombination for efficient perovskite leds, *Nature* **630**, 631 (2024).
 - [7] L. Kong, Y. Luo, Q. Wu, X. Xiao, Y. Wang, G. Chen, J. Zhang, K. Wang, W. C. Choy, Y.-B. Zhao, *et al.*, Efficient and stable hybrid perovskite-organic light-emitting diodes with external quantum efficiency exceeding 40 per cent, *Light: Science & Applications* **13**, 138 (2024).
 - [8] A. Fakhruddin, M. K. Gangishetty, M. Abdi-Jalebi, S.-H. Chin, A. R. bin Mohd Yusoff, D. N. Congreve, W. Tress, F. Deschler, M. Vasilopoulou, and H. J. Bolink, Perovskite light-emitting diodes, *Nature Electronics* **5**, 203 (2022).
 - [9] Q. Dong, L. Lei, J. Mendes, and F. So, Operational stability of perovskite light emitting diodes, *Journal of Physics: Materials* **3**, 012002 (2020).
 - [10] Y. Jia, H. Yu, Y. Zhou, N. Li, Y. Guo, F. Xie, Z. Qin, X. Lu, and N. Zhao, Excess ion-induced efficiency roll-off in high-efficiency perovskite light-emitting diodes, *ACS Applied Materials & Interfaces* **13**, 28546 (2021).

- [11] P. R. Nair and K. Raitani, Photoluminescence efficiency droop in perovskites, *ACS Photonics* (2024).
- [12] S. Agarwal, M. Seetharaman, N. K. Kumawat, A. S. Subbiah, S. K. Sarkar, D. Kabra, M. A. Namboothiry, and P. R. Nair, On the uniqueness of ideality factor and voltage exponent of perovskite-based solar cells, *Journal of Physical Chemistry Letters* **5**, 4115 (2014).
- [13] V. Nandal and P. R. Nair, Predictive modeling of ion migration induced degradation in perovskite solar cells, *ACS Nano* **11**, 11505 (2017), pMID: 29099174.
- [14] K. Hossain, D. Sivadas, D. Kabra, and P. R. Nair, Perovskite solar cells dominated by bimolecular recombination how far is the radiative limit?, *ACS Energy Letters* **9**, 2310 (2024).
- [15] R. F. Pierret, *Advanced Semiconductor Fundamentals* (Addison-Wesley Longman Publishing Co., Inc., USA, 1987).
- [16] W. van Roosbroeck and W. Shockley, Photon-radiative recombination of electrons and holes in germanium, *Phys. Rev.* **94**, 1558 (1954).
- [17] C. L. Davies, M. R. Filip, J. B. Patel, T. W. Crothers, C. Verdi, A. D. Wright, R. L. Milot, F. Giustino, M. B. Johnston, and L. M. Herz, Bimolecular recombination in methylammonium lead triiodide perovskite is an inverse absorption process, *Nature Communications* **9**, 293 (2018).
- [18] E. A. Duijnste, J. M. Ball, V. M. Le Corre, L. J. A. Koster, H. J. Snaith, and J. Lim, Toward understanding space-charge limited current measurements on metal halide perovskites, *ACS Energy Letters* **5**, 376 (2020).
- [19] V. M. Le Corre, E. A. Duijnste, O. El Tambouli, J. M. Ball, H. J. Snaith, J. Lim, and L. J. A. Koster, Revealing charge carrier mobility and defect densities in metal halide perovskites via space-charge-limited current measurements, *ACS energy letters* **6**, 1087 (2021).
- [20] E. A. Duijnste, V. M. Le Corre, M. B. Johnston, L. J. A. Koster, J. Lim, and H. J. Snaith, Understanding dark current-voltage characteristics in metal-halide perovskite single crystals, *Physical review applied* **15**, 014006 (2021).
- [21] J. Yu, H. Hanafusa, and S. Higashi, Extraction of interfacial thermal resistance across an organic/semiconductor interface using optical-interference contactless thermometry, *Applied Physics Express* **17**, 036502 (2024).
- [22] L. Zhao, K. Roh, S. Kacmoli, K. Al Kurdi, S. Jhulki, S. Barlow, S. R. Marder, C. Gmachl, and B. P. Rand, Thermal management enables bright and stable perovskite light-emitting diodes, *Advanced Materials* **32**, 2000752 (2020).
- [23] S. Zheng, Z. Wang, N. Jiang, H. Huang, X. Wu, D. Li, Q. Teng, J. Li, C. Li, J. Li, *et al.*, Ultralow voltage-driven efficient and stable perovskite light-emitting diodes, *Science Advances* **10**, eadp8473 (2024).
- [24] P. R. Nair, Near ideal photoluminescence in perovskites: Excitonic effects and self-consistent back extraction of recombination parameters, *Journal of Applied Physics* **137**, 083104 (2025).
- [25] P. R. Nair, Near ideal photoluminescence in perovskites: Excitonic effects and self-consistent back extraction of recombination parameters, *Journal of Applied Physics* **137** (2025).
- [26] W. Bai, T. Xuan, H. Zhao, H. Dong, X. Cheng, L. Wang, and R.-J. Xie, Perovskite light-emitting diodes with an external quantum efficiency exceeding 30%, *Advanced Materials* **35**, 2302283 (2023).
- [27] G. V. Chittiboina, A. Singareddy, A. Agarwal, S. Bhatta, and P. R. Nair, Intrinsic degradation-dependent energy yield estimates for perovskite/silicon tandem solar cells under field conditions, *ACS Energy Letters* **8**, 2927 (2023).
- [28] S. Agarwal and P. R. Nair, Device engineering of perovskite solar cells to achieve near ideal efficiency, *Applied Physics Letters* **107**, 123901 (2015).
- [29] A. Singareddy, U. K. R. Sadula, and P. R. Nair, Phase segregation induced efficiency degradation and variability in mixed halide perovskite solar cells, *Journal of Applied Physics* **130**, 10.1063/5.0062818 (2021), 225501.